*Proc. Natl. Acad. Sci. USA*
Vol. 93, pp. 7337–7340, July 1996
Neurobiology

# Selective expression of m2 muscarinic receptor in the parvocellular channel of the primate visual cortex

**(striate cortex/synapses/neurotransmission/neuromodulation/heteroreceptor)**

LADISLAV MRZLJAK*†, ALLAN I. LEVEY‡, AND PASKO RAKIC*

*Section of Neurobiology, Yale University School of Medicine, New Haven, CT 06511; and ‡Department of Neurology, Emory University School of Medicine, Atlanta, GA 30322

*Contributed by Pasko Rakic, March 20, 1996*

**ABSTRACT** **Visual information in primates is relayed from the dorsal lateral geniculate nucleus to the cerebral cortex by three parallel neuronal channels designated the parvocellular, magnocellular, and interlaminar pathways. Here we report that m2 muscarinic acetylcholine receptor in the macaque monkey visual cortex is selectively associated with synaptic circuits subserving the function of only one of these channels. The m2 receptor protein is enriched both in layer IV axons originating from parvocellular layers of the dorsal lateral geniculate nucleus and in cytochrome oxidase poor interblob compartments in layers II and III, which are linked with the parvocellular pathway. In these compartments, m2 receptors appear to be heteroreceptors, i.e., they are associated predominantly with asymmetric, noncholinergic synapses, suggesting a selective role in the modulation of excitatory neurotransmission through the parvocellular visual channel.**

Information processing within the mammalian visual system involves three functional parallel pathways that remain segregated from the retina to the visual cortex. Two of these pathways, the so-called M and P pathways, originate from the magno- and parvocellular layers, respectively, of the dorsal lateral geniculate nucleus of the thalamus and are involved in motion, color, and form discrimination (1, 2). The third pathway, known as the I or K channel, originates from neurons in interlaminar regions or the koniocellular layers of the lateral geniculate nucleus (3–5). In the primary visual cortex of macaque monkeys, information carried by M, P, and K channels is partitioned in the subdivisions of layer IV and among cytochrome oxidase (CO)-rich blob (puff) and interblob (interpuff) compartments of layers II and III. The P pathway axons terminate in layers IVA and IVCb, and M pathway axons terminate in layer IVCa (6). The K channel axons project directly to the CO-rich blobs, whereas the M and P channels form indirect projections to both blobs and interblobs (4, 5). Although a number of peptides and neurotransmitters, as well as their synthesizing enzymes and receptors, are distributed differentially within these compartments in the primary visual cortex, none has been shown to be selectively associated with the specific synaptic circuits of only one visual channel (7–11). Here, using antibodies generated against the recombinant m2 receptor subtype (12, 13) in combination with light and electron microscopic immunohistochemistry and CO histochemistry, we report that m2 muscarinic acetylcholine receptor immunoreactivity is enriched in the P channel of the primary visual cortex in macaque monkey.

Muscarinic receptors mediate in large part the action of acetylcholine (14), the neurotransmitter that has been shown to have important modulatory functions within the visual cortex (14, 15). Recent cloning of muscarinic receptor genes *m1-m5* (16) and the production of subtype-specific antibodies against receptor proteins (12, 13) have allowed the localization of individual receptors with high specificity at both the light and electron microscopic levels (12, 17). We have taken advantages of these advances to examine the expression of the m2 receptor protein in circuits of the primary visual cortex in the macaque monkeys.

## MATERIALS AND METHODS

Five adult rhesus monkeys (*Macaca mulatta*), housed and treated in accordance with institutional guidelines, were employed in this study. The animals were deeply anesthetized with Nembutal (100 mg/kg given intravenously) and perfused through the heart with 3–4% paraformaldehyde/0.1% glutaraldehyde/0.2% picric acid in 0.1 M phosphate buffer. Coronal or tangential blocks of the primary visual cortex area were cut frozen at 30–40 μm on a cryostat for light microscopic examination or on a vibratome for electron microscopic analysis. Adjacent sections were processed both for immunohistochemistry by use of subtype-specific polyclonal (12) or monoclonal (13) antibodies against recombinant m2 receptor protein and CO histochemistry (18). Sections were photographed and examined with a Zeiss Aristoplan microscope. For electron microscopic analysis, vibratome sections stained for m2 receptor were first osmicated in 1–2% osmium tetroxide in phosphate buffer and flat embedded in Durcupan (Fluka). Selected blocks were cut serially into ultrathin sections on an Ultramicrotome (Reichert), stained with lead citrate and uranyl acetate, and examined with a JEOL transmission electron microscope.

The quantification of m2-positive structures (e.g., axons and dendrites) in m2-rich interblobs was performed on electron micrographs as described (19, 20). The analysis was performed on sections obtained from three blocks in one representative monkey case. Electron micrographs (500) from the interblob area in the superficial and deep parts of layer III were printed at a final magnification of ×25,000. The total interblob area analyzed was 30,390 $\mu m^2$, and in the quantitative assessment we determined (*i*) the frequency of m2-positive tissue elements (e.g., axons and dendrites) and (*ii*) the labeling index for each element by dividing the percentage of each m2-positive element by the percentage of element (total labeled and unlabeled) in our sample. The latter information was obtained by randomly superimposing the grid with 63 crossing points on each micrograph.

## RESULTS

In the monkey visual cortex, we found the strongest m2 immunoreactivity in layers IVA and IVCb (Figs. 1*A* and 2

The publication costs of this article were defrayed in part by page charge payment. This article must therefore be hereby marked "*advertisement*" in accordance with 18 U.S.C. §1734 solely to indicate this fact.

Abbreviations: CO, cytochrome oxidase; GABA, aminobutyric acid.

†To whom reprint requests should be addressed at: Section of Neurobiology, Yale School of Medicine, 333 Cedar Street, New Haven, CT 06510. e-mail: ladislav.mrzljak@yale.edu.

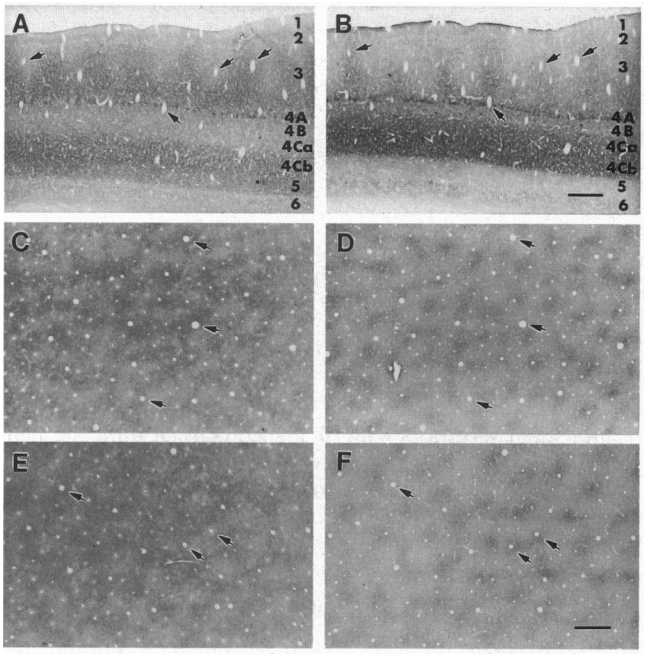


FIG. 1. Adjacent coronal (*A* and *B*) and tangential (*C–F*) sections processed for m2 receptor immunohistochemistry (*A*, *C*, and *E*) and CO histochemistry (*B*, *D*, and *F*). Sections in *C* and *D* are through superficial strata of layer III, and sections in *E* and *F* are through deep strata of layer III. Note interdigitation between the m2 receptor and CO; m2-rich compartments occupy CO-poor interblob areas. Arrows point to blood vessels in the adjacent sections that are used as markers for alignment. In coronal sections (*A* and *B*), m2-rich staining in parvocellular recipient layers 4A and 4Cb and intense CO reactivity overlap. In contrast, m2 immunoreactivity is poor in the magnocellular layers IVCa and IVB and abundant in layer V, which is inverse to the pattern of CO staining. [*B*, bar = 300 μm (for *A* and *B*); *F*, bar = 0.5 mm (for *C–F*).]

*C–F*). The stained elements form a dense network of fibers that bear numerous boutons, whose shape and ultrastructure are consistent with the terminations of the P pathway (6). As observed in the electron microscope, these large immunoreactive boutons (>1 μm) form multiple asymmetric synapses, predominantly on dendritic spines and less commonly on dendritic shafts and cell bodies of cortical neurons (Fig. 3 *C* and *D*).

Further evidence for selective enrichment of m2 receptor in the P channel comes from enriched staining in the CO-poor interblob compartments, which receive intracortical projections from layer IVCb neurons, which belong to the P system in the visual cortex (21, 22). An examination of coronal sections through the macaque primary visual cortex revealed the presence of distinct, vertically oriented m2 receptor-enriched compartments within layers II and III that alternate with the m2-poor zones (Fig. 1*A*). Adjacent CO-stained sections show that m2-rich zones correspond to the CO-poor interblob regions (Fig. 1*B*). Tangential sections cut parallel to the pial surface of the primary visual cortex revealed the pattern of interdigitation of m2 and CO staining; m2 receptor immunoreactivity forms a matrix with round, poorly immunostained holes into which CO blobs fit precisely (Figs. 1 *C–F* and 4). Electron microscopic analysis revealed that m2-enriched, diffuse granular interblob neuropil (Fig. 2 *A* and *B*) contained both immunopositive axons (Fig. 3 *A* and *B*), as well as dendrites and spines (Fig. 5 *A* and *B*). The labeled axons typically formed asymmetric synapses with spines and small dendrites (Fig. 3 *A* and *B*). In addition, a smaller number of axons forming symmetric junctions, with all characteristics of cholinergic afferents in the cortex (23), was also observed.

Quantitative analysis revealed that, among m2-positive elements in interblobs, axonal labeling accounts for 55.2% of

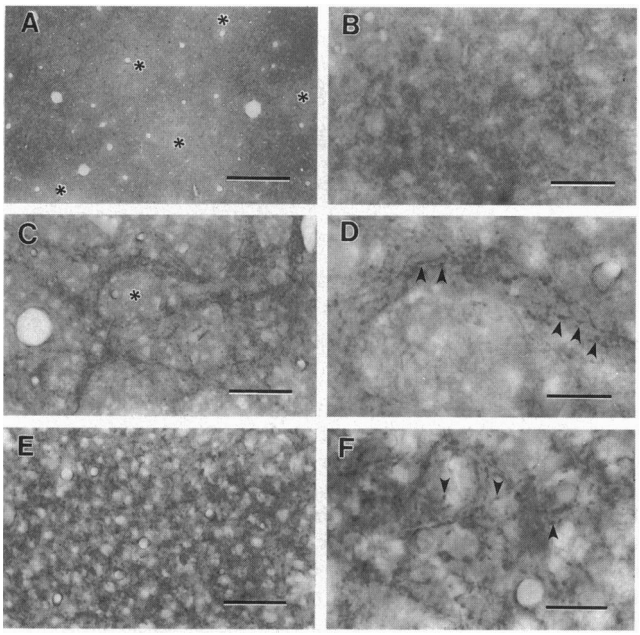


FIG. 2. Low and high magnification photomicrographs of tangential sections through m2-rich and m2-poor (asterisks) compartments in layer III (*A* and *B*), honeycomb-like m2 immunoreactivity of layer IVA (*C* and *D*), and dense staining in layer IVCb (*E* and *F*). In contrast to diffuse and granular neuropil in m2-rich compartments of layer III (*A* and *B*), staining in layers IVA and IVCb consists of immunopositive fibers that bear numerous boutons characteristic for P axonal terminals (arrowheads in *D* and *F*). (*A*, *C*, and *E*, bar = 200 μm; *B*, *D*, and *F*, bar = 40 μm.)

elements (axon terminals forming asymmetric synapses, 23.8%; symmetric contacts, 9.4%; and without visible synaptic contact, 22%). Dendrites were found in 17.8%, spines in 6.6%, and unidentified profiles in 20,4% of labeled elements. Axons forming asymmetric and symmetric synapses had the largest

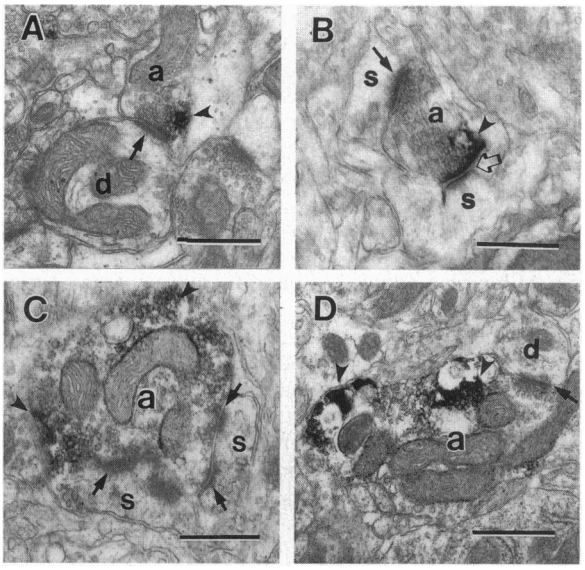


FIG. 3. (*A* and *B*) Two m2-positive axons (a) in m2-rich layer III interblob domains form asymmetric synapses (arrows) with a dendrite (d) (*A*) and two spines (s) (*B*). Arrowheads point to immunoreaction product either segregated from (*A*, *C*, and *D*) or associated with (*B*, open arrow) the synaptic specializations. In comparison with positive axons in m2-rich compartments of layers II and III (*A* and *B*), those in layers IVA (*C*) and IVCb (*D*) are larger (>1 μm). They form multiple synaptic contacts with dendritic spines (arrows, *C*) and small dendrites (*D*), characteristic of P terminals. (Bars = 0.5 μm.)

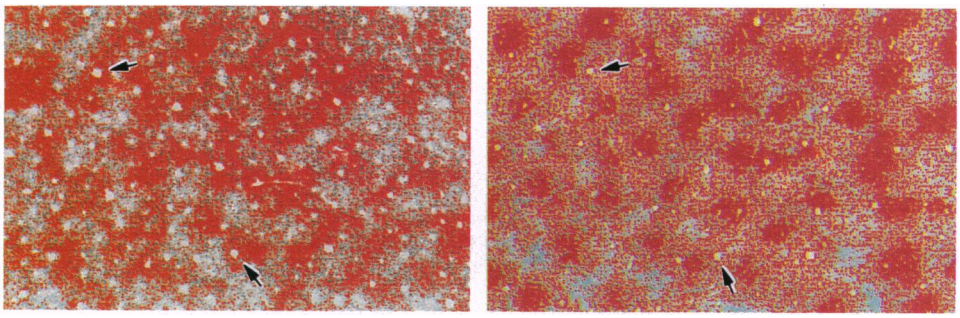

FIG. 4. Computer pseudo-colored images of micrographs shown in Fig. 1 *E* and *F* generated for better visualization of complementary of m2 (*Left*) and CO (*Right*).

labeling indexes, 3.4 and 4.7, respectively. The labeling indexes for spines and unidentified profiles were 1.2 and 1.7, respectively. Although dendritic profiles were most frequently encountered in our sample (44.3%), they were least frequently labeled (labeling index 0.4%).

## DISCUSSION

We present new evidence for chemical specialization within a thalamocortical pathway in the primate visual system. Among three parallel channels, which relay visual information from the lateral geniculate nucleus, m2 muscarinic acetylcholine receptor is selectively enriched in the P pathway in the macaque primary visual cortex. Thus, we found strong m2 immunoreactivity in CO-poor interblob compartments of layers II and III, as well as layers IVA and IVCb, that are associated with the P stream. In contrast, m2 receptor protein expression in CO-rich blob compartment and layer IVCa, which receive K and M pathway projections, respectively, is sparse. The m2-positive terminals in layers IVA and IVCb are defined as parvocellular by established criteria based on tracing experiments at the light and electron microscopic levels. (*i*) P axons terminate in sublayers IVA and IVCb (6), and (*ii*) these terminal are large and form usually multiple asymmetric synapses predominantly with spines (24, 25).

**Origin of m2 Immunoreactive Circuitry in Interblobs.** Although both presynaptic and postsynaptic m2-positive elements contribute to the enriched immunostaining in the interblob compartments of the layers II and III, m2-positive axons forming asymmetric synapses are most numerous. These axons presumably belong to spiny stellate and pyramidal neurons of the P layers, which are known to project to interblobs (21, 22), where they form asymmetric synapses (26). Casagrande and coworkers (21) found that the majority of these interblob projection neurons are situated in the IVCb P layer. In contrast, Yoshioka and coworkers (22) pointed out that spiny stellate neurons, which project to interblob regions, are situated at the border between layers IVCa and IVCb and, therefore, should carry both M and P channel information. However, since layer IVCa exhibits poor m2 staining, it is unlikely that M neurons contribute to m2-rich staining in the interblobs. Other possible, but less likely, candidates for the origin of m2-positive interblob axons are neurons of the secondary visual areas (27). The origin of asymmetric input may also be from the intralaminar and central thalamic nuclei (28), as well as the serotoninergic fiber network of the brain stem (29).

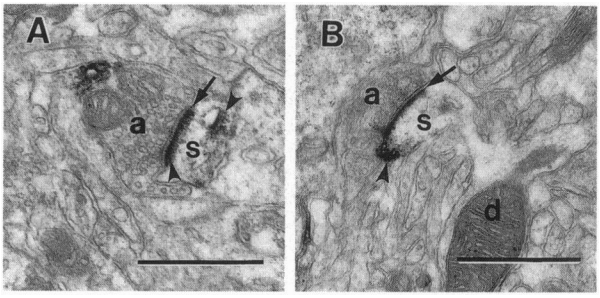


FIG. 5. Postsynaptic localization of m2 receptor in m2-rich interblobs (*A* and *B*). Two immunoreactive spines (s) are postsynaptic elements of asymmetric synapses (arrows) formed by unlabeled axons (a). Although the immunoreactivity is present on the postsynaptic densities (arrowheads), due to the diffusion of immunoperoxidase end-product, this localization may be also be the result of secondary depositions of immunoreaction label from extrasynaptic sites in the dendritic spines. (Bars = 0.5 μm.)

If m2-positive axons forming asymmetric synapses in interblobs belong to the neurons in P layer IVCb, it would be expected that these neurons synthesize the m2 receptor protein. Also, the presence of immunoreactive dendrites and spines in interblobs is additional evidence that selected neurons in the primary visual cortex may synthesize this receptor. It may be surprising that no m2 immunoreactive neuronal somata were observed in layer IVC and very few m2-positive, presumably GABAergic, neurons are found in other layers of the primary visual cortex. The absence of m2-positive somata may be due to the selectivity of our antibody, which recognizes only the mature form of the receptor at functionally active sites. The m2 protein is presumably synthesized by neurons situated outside the interblobs and then transported and accumulated in distal dendrites, dendritic spines, and axon terminals, which reside in the interblobs. Spiny stellate neurons in layer IV or pyramidal neurons in the infragranular layers are the most likely candidates for synthesis and the selective distribution of m2 receptor protein within the interblobs because parts of their distal dendrites and axons reside in this region (26, 30). Indeed, our preliminary data about localization of mRNA for the m2 receptor in the macaque visual cortex (data obtained by *in situ* hybridization histochemistry; data not shown) suggest the presence of m2-synthesizing neurons in the infragranular layers, as well as in layer IV.

The smaller proportions of m2-positive terminals in the interblobs form symmetric synapses and presumably belong to cholinergic axons because cholinergic axons in the primate, carnivore, and rodent neocortex form exclusively symmetric synapses (23, 31, 32) and their neurons of origin in the basal forebrain synthesize m2 receptor protein (13). In cholinergic axons, m2 receptors function as autoreceptors, which inhibit acetylcholine release (33). Cholinergic axons are present in the interblob areas, although no periodic differences in their density is observed in supragranular layers (34, 35). Another potential source of m2-positive fibers forming symmetric synapses in the cerebral cortex are GABAergic neurons in the basal forebrain (36), which also express m2 protein (13). In contrast, the asymmetric type of synapses in the cerebral cortex belong predominantly to thalamo-cortical and cortico-cortical pathways, which use excitatory amino acids as neurotransmitters (37).

**Function and Significance of m2 Receptor Localization.** Localization of the m2 receptor in both presynaptic and

postsynaptic elements of noncholinergic asymmetric synapses suggests its role as a heteroreceptor in the visual cortex, as it has been shown in some other cortical areas (17). For example, presynaptic m2 heteroreceptors in the interblobs and in the P axons of layer IV may regulate the release of glutamate, the principal neurotransmitter in cortico-cortical and thalamocortical projections, including the visual afferent pathways (11, 38, 39). For example, stimulation of presynaptic m2 heteroreceptors in the neocortex reduces glutamate release from nerve terminals and modifies excitatory postsynaptic potentials (40). In the primary visual cortex, cholinergic agonists reduce the amplitude of the fast excitatory postsynaptic potentials via presynaptic mechanisms involving muscarinic receptors (41). An additional mechanism suggested by our results is that m2 heteroreceptors situated on spines and dendrites may modify such inputs at the postsynaptic level. The acetylcholine, which activates m2 heteroreceptors, may diffuse from local cholinergic fiber networks (32) that are in close nonjunctional contact with glutamate-positive axons and spines (42). Therefore, these heteroreceptor mechanisms may not involve cholinergic synapses but rather "volume transmission" (43). Our findings suggest that the m2 receptor may modulate input and output information within the interblobs via m2 receptors. Interblob neurons belong to the so called "infratemporal" stream, which is in the visual cortical hierarchy responsible for object recognition (1, 2). The interblob neurons are orientation-selective and binocularly driven and have no color preference (1). It is generally accepted that the neurotransmitter $\gamma$-aminobutyric acid (GABA) is involved in modulation of orientation specificity and other receptive field properties, i.e., functions represented in interblobs (44). It was also suggested that the cholinergic system may be implicated in this modulation by bringing inhibitory GABAergic circuitry to a level of activity where it becomes effective (45). Such cholinergic–GABAergic interaction may be implemented via both pre- and postsynaptic muscarinic receptors. For example, acetylcholine can directly excite GABA neurons in the visual cortex via postsynaptic muscarinic receptors (46) or inhibit excitatory synaptic transmission through presynaptic muscarinic receptors (40, 41).

In conclusion, our results show that m2 receptor immunohistochemistry can serve as a useful marker for the P pathway within the primate primary visual cortex. Furthermore, the pattern of distribution of m2 receptor protein in cortical circuitry suggests its modulatory function in segregated visual pathways.

We are grateful to Drs. P. S. Goldman-Rakic, S. Hendry, M. Schwartz, and K. Wikler for comments on the manuscript and M. Pappy and J. Musco for technical assistance. This work was supported by U.S. Public Health Service Grants EY 02593 and MH 44866.

1. Livingstone, M. & Hubel, M. (1988) *Science* **240,** 740–749.
2. Van Essen, D. C. & Gallant, J. L. (1994) *Neuron* **13,** 1–10.
3. Fitzpatrick, D., Itoh, K. & Diamond, I. T. (1983) *J. Neurosci.* **3,** 673–702.
4. Hendry, S. H. C. & Yoshioka, T. (1994) *Science* **264,** 575–577.
5. Casagrande, V. A. (1994) *Trends Neurosci.* **17,** 305–310.
6. Hendrickson, A. E., Wilson, J. R. & Ogren, M. P. (1978) *J. Comp. Neurol.* **182,** 123–136.
7. Hendrickson, A. E., Hunt, S. P. & Wu, J.-Y. (1981) *Nature (London)* **292,** 605–607.
8. Celio, M. R., Scharer, L., Morrison, J. H., Norman, A. W. & Bloom, F. E. (1986) *Nature (London)* **323,** 715–717.
9. Hendry, S. H. C., Schwark, H. D., Jones, E. G. & Yan, J. (1987) *J. Neurosci.* **7,** 1503–1519.
10. Hendry, S. H., Huntsman, M. M., Vinuela, A., Mohler, H., De Blas, A. L. & Jones, E. G. (1994) *J. Neurosci.* **14,** 2383–2401.
11. Carder, R. K. & Hendry, S. H. (1994) *J. Neurosci.* **14,** 242–262.
12. Levey, A. I., Kitt, C. A., Simonds, W. F., Price, D. L. & Brann, M. R. (1991) *J. Neurosci.* **11,** 3218–3226.
13. Levey, A. I., Edmunds, S. M., Hersch, S. M., Wiley, R. G. & Heilman, C. J. (1995) *J. Comp. Neurol.* **351,** 339–356.
14. Sillito, A. M. & Kemp, J. A. (1996) *Brain Res.* **289,** 143–155.
15. McCormick, D. A. (1992) *Prog. Neurobiol.* **39,** 337–388.
16. Bonner, T. I., Buckley, N. J., Young, A. C. & Brann, M. R. (1987) *Science* **237,** 527–532.
17. Mrzljak, L., Levey, A. I. & Goldman-Rakic, P. S. (1993) *Proc. Natl. Acad. Sci. USA* **90,** 5194–5198.
18. Wong-Riley, M. T. T. (1979) *Brain Res.* **171,** 11–28.
19. Williams, M. A. (1969) in *Advances in Optical and Electron Microscopy*, eds. Barer, R. & Coslett, V. E. (Academic, New York), Vol. 3, pp. 219–272.
20. Schwartz, M. L., Dekker, J. J. & Goldman-Rakic, P. S. (1991) *J. Comp. Neurol.* **309,** 289–304.
21. Lachica, E. A., Beck, P. D. & Casagrande, V. A. (1992) *Proc. Natl. Acad. Sci. USA* **89,** 3566–3570.
22. Yoshioka, T., Levitt, J. B. & Lund, J. S. (1994) *Visual Neurosci.* **11,** 467–489.
23. Mrzljak, L., Pappy, M., Leranth, C. & Goldman-Rakic, P. S. (1995) *J. Comp. Neurol.* **357,** 603–617.
24. Winfield, D. A., Rivera-Dominguez, M. & Powell, T. P. S. (1982) *Brain Res.* **231,** 19–32.
25. Freund, T. F., Martin, K. A., Soltesz, I., Somogyi, P. & Whitteridge, D. (1989) *J. Comp. Neurol.* **289,** 315–336.
26. Blasdel, G. G., Lund, J. S. & Fitzpatrick, D. (1985) *J. Neurosci.* **5,** 3350–3369.
27. Rockland, K. S. (1994) in *Cerebral Cortex: Primary Visual Cortex in Primates*, eds. Peters, A. & Rockland, K. (Plenum, New York), Vol. 10, pp. 261–299.
28. Doty, R. W. (1983) *J. Comp. Neurol.* **218,** 159–173.
29. de Lima, A. D., Bloom, F. E. & Morrison, J. H. (1988) *J. Comp. Neurol.* **274,** 280–294.
30. Peters, A. & Sethares, C. (1991) *J. Comp. Neurol.* **306,** 1–23.
31. de Lima, A. D. & Singer, W. (1986) *J. Comp. Neurol.* **250,** 324–338.
32. Umbriaco, D., Watkins, K. C., Descarries, L., Cozzari, C. & Hartman, B. K. (1994) *J. Comp. Neurol.* **348,** 351–373.
33. Pohorecki, R., Head, R. & Domino, E. F. (1988) *J. Pharmacol. Exp. Ther.* **244,** 213–217.
34. Mrzljak, L. & Goldman-Rakic, P. S. (1993) *Cereb. Cortex* **3,** 133–147.
35. Mesulam, M. M., Hersch, L. B., Mash, D. C. & Geula, C. (1992) *J. Comp. Neurol.* **318,** 316–328.
36. Freund, T. F. & Meskenaite, V. (1992) *Proc. Natl. Acad. Sci. USA* **89,** 738–742.
37. Conti, F., DeFelipe, J., Farinas, I. & Manzoni, T. (1989) *J. Comp. Neurol.* **290,** 141–153.
38. Baughman, R. W. & Gilbert, C. D. (1981) *J. Neurosci.* **1,** 427–439.
39. Kisvarday, Z. F., Cowey, A., Smith, A. D. & Somogyi, P. (1989) *J. Neurosci.* **9,** 667–682.
40. Vidal, C. & Changeux, J. P. (1993) *Neuroscience* **56,** 23–32.
41. Murakoshi, T. (1995) *Vision Res.* **35,** 25–35.
42. Aoki, C. & Kabak, S. (1992) *Visual Neurosci.* **8,** 177–191.
43. Agnati, L. F., Zoli, M., Stromberg, I. & Fuxe, K. (1995) *Neuroscience* **69,** 711–726.
44. Sillito, A. M. (1992) *Prog. Brain Res.* **90,** 349–384.
45. Sillito, A. M. (1993) *Prog. Brain Res.* **98,** 371–378.
46. McCormick, D. A. & Prince, D. A. (1985) *Proc. Natl. Acad. Sci. USA* **82,** 6344–6348.